processes

MDPI

Article

The Application of Rotary Twist Collecting Actuator Systems for *Camellia oleifera* Flower Bud Collection

Qing Zhao, Lijun Li * and Zhifeng Yang

Engineering Research Center for Forestry Equipment of Hunan Province, Central South University of Forestry and Technology, Changsha 410004, China; zhaoqing@csuft.edu.cn (Q.Z.); 20211294@csuft.edu.cn (Z.Y.)
* Correspondence: t20120466@csuft.edu.cn

Abstract: Pollen transmission of *Camellia oleifera* is affected by climate and environment, and the quality of natural pollination is not high, which seriously affects the yield of *Camellia oleifera*. Artificial pollination is an effective way to solve the low fruit setting rate of natural pollination, but the problem to be solved urgently in artificial pollination is the collection of a large amount of pollen. At present, there is no mechanized equipment for *Camellia oleifera* flower bud collection, so developing an efficient pollen collection device has become a key problem that restricts the high-quality development of *Camellia oleifera*. In this paper, on the basis of measuring the tensile force, the shearing force, and the torsional moment required to remove Camellia Oleifera flower bud from the branch, which are 8.968 N, 13.94 N, and 0.0178 N·m, respectively, three types of *Camellia oleifera* flower bud collecting actuators were designed. According to the results of parameter design, feasibility analysis, and dynamic simulation, the power parameters of three types of *Camellia oleifera* flower bud collecting actuators were obtained. The experiment of collecting *Camellia oleifera* flower bud was designed, and the collection time, collection rate, and bud breakage rate of the three collecting actuators were compared. The experimental results show that the collection time of the rotary twist-type collecting actuator was 1.57 s, the collection rate was 91%, and the breakage rate was 4.9%, which can realize the efficient and low-loss collection of *Camellia oleifera* flowers bud, providing a theoretical basis for subsequent research on a *Camellia oleifera* flower bud collection robot.

Keywords: *Camellia oleifera*; flower bud collecting; rotary twist; triple-finger linkage; shear type

Citation: Zhao, Q.; Li, L.; Yang, Z. The Application of Rotary Twist Collecting Actuator Systems for *Camellia oleifera* Flower Bud Collection. *Processes* **2024**, *12*, 1023. https://doi.org/10.3390/pr12051023

Academic Editor: Diane Mynors

Received: 17 April 2024
Revised: 14 May 2024
Accepted: 15 May 2024
Published: 17 May 2024

1. Introduction

Camellia oleifera is a unique woody oil edible tree in China. At present, *Camellia oleifera* pollination is mainly based on natural insects. From November to December every year is the flowering period of *Camellia oleifera*, when the temperature is low insect activity is low, the natural pollination quality is not high, which seriously affects the yield of *Camellia oleifera*. Artificial pollination requires the collection of a large number of *Camellia oleifera* flower bud to extract pollen, but artificial collection is inefficient and labor-intensive [1,2]. Mechanized flower bud collection of *Camellia oleifera* can solve the problem of the low efficiency of manual flower bud collection and reduce the limitation of natural factors on pollen resources [3,4].

American scholar Vangeyte and others [5] have developed a chrysanthemum picker. The picking actuator consists of movable picking fingers and a drum. The drum pulls the chrysanthemum into the drum, cleans the chrysanthemum with a brush, brushes it off with a comb knife and, finally, collects it with a conveyor belt. However, the comb knife will destroy the flower bud during its work. Chinese scholar Wang Jiaze [6] studied the rose collecting actuator with integrated cutting and clamping. When working, the clamping jaw opens and then closes with the tool rest. The blade cuts off the stem of the rose and then clamps the rose to complete the picking action. However, the actuator requires high positioning accuracy, so it is difficult to achieve efficient collection.

In this study, based on the consideration of tensile force, shear force, and torsional moment, three types of *Camellia oleifera* flower bud collecting actuators were designed. On the basis of structural design and feasibility analysis, prototype collecting experiments were carried out to verify the working performance of the rotary-twist actuator.

2. Problem

The biomechanical properties of *Camellia oleifera* flower bud are the basis for the design of the collecting actuator. The diameter and length of *Camellia oleifera* flower bud determine the shape of the collecting actuator, and the tensile, shear, and torsional moments that separate the *Camellia oleifera* flower bud from the branches and trunks determine the working principle of the collecting actuator. Hua Shuo, Hua Jin, and Hua Xin (hereinafter referred to as "San Hua"), which have the largest cultivated area in the hilly areas of China, were taken as the object of observation. The opening of *Camellia oleifera* flower bud includes four periods, including bud cracking, first opening, petal standing, and petal falling, as shown in Figure 1.

(**a**) (**b**) (**c**) (**d**)

Figure 1. Four flowering periods of the *Camellia oleifera* flower:(**a**), bud cracking, (**b**) initial opening, (**c**) petal standing, and (**d**) petal falling.

In this study, we studied *Camellia oleifera* flower bud in the first three periods, with the highest pollen activity. Ten *Camellia oleifera* trees were randomly chosen, and 10 flower bud were taken from each tree. The diameter, length, and mass were measured in groups of 10×10, and the average value of the three periods was recorded. The measurement method is shown in Figure 2a. The flower bud quality was measured by a precision electronic balance with a weighing range of 0–100 g and a repeatability error of 0.01 g. The length of the flower bud was measured by an ordinary vernier caliper. The measurement results are shown in Table 1.

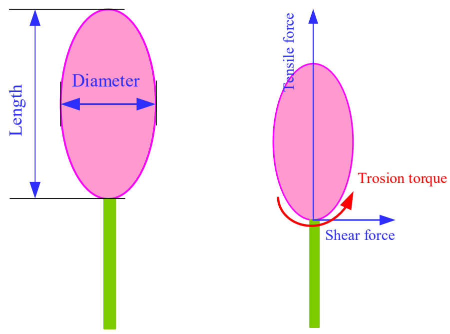

(**a**) (**b**)

Figure 2. Dimension schematic and force schematic of *Camellia oleifera* flower bud: (**a**) dimension schematic, and (**b**) force schematic.

Table 1. Botanical characteristics of "SanHua Series" *Camellia oleifera* flower bud.

Group No.	Diameter/mm			Length/mm			Quality/g		
Flowers Period	**Bud Cracking**	**Initial Opening**	**Petal Standing**	**Bud Cracking**	**Initial Opening**	**Petal Standing**	**Bud Cracking**	**Initial Opening**	**Petal Standing**
1	18.21 [1]	26.83	74.36	26.27	29.3	22.16	1.85	2.15	1.79
2	17.7	28.52	79.52	26.48	29.82	22.16	1.84	2.04	1.99
3	17.53	28.29	77.3	25.44	30.22	23.2	1.98	1.98	1.85
4	17.66	31.2	79.76	26.37	29.18	21.32	1.76	2.22	1.73
5	18.34	29.03	73.24	27.99	29.64	21.84	1.86	2.12	2.01
6	19.15	29.08	80.26	26.67	29.55	21.64	1.95	1.95	2.12
7	18.15	32.89	74.64	25.47	29.54	21.78	1.9	1.9	1.76
8	17.63	31.34	77.4	27.16	31.37	20.96	1.79	2.16	1.87
9	19.04	32.28	75.78	26.65	29.73	20.92	1.86	2.09	1.75
10	18.89	29.79	82.9	26.38	30.85	22.78	1.75	2.14	1.85
Average	18.23 [2]	29.93 [2] 41.89 [3]	77.52 [2]	26.49 [2]	29.92 [2] 26.10 [3]	21.88 [2]	1.85 [2]	2.08 [2] 1.93 [3]	1.87 [2]

[1] Each measurement in the table is the average of 10 *Camellia oleifera* flower measurements from the same tree in this flowering period. [2] The average value is the average value of data from the column of flowering periods 1 to 10. [3] The average value is the average of the data in three periods from the previous column. The diameter was 41.89 mm, the length was 26.10 mm, and the mass was 1.93 g.

2.1. Botanical Characteristics of Camellia oleifera Flower Bud

Camellia oleifera belongs to small evergreen trees, with flourishing branches and good toughness. Generally, lush branches and leaves grow around the flower bud, and the bud does not fall off easily without great tensile force or shear force.

The manner in which the flower bud are separated from the branches is an essential factor in the design of the collecting actuator. The *Camellia oleifera* flower bud were tested for longitudinal tensile force, transverse shear, and torsional moment. The transverse shear acted on the flower stem at the bottom, which had nothing to do with the flowering period, so the transverse shear did not affect the flowering period. The measurement method is shown in Figure 2b. The tensile force and shear force of *Camellia oleifera* flower bud were measured by a Sanliang brand SL-300 model mechanical measuring instrument with an accuracy of 0.1 N. The torsional moment of *Camellia oleifera* flower bud was measured by an HP-10 digital display torsion tester with accuracy of 0.001 N.m.

The experimental process is shown in Figure 3, and the bud separated from the branches all maintained the appearance integrity.

(**a**) (**b**) (**c**)

Figure 3. Biomechanical property measurement test of *Camellia oleifera* flower bud: (**a**) tensile force test, (**b**) shear force test, and (**c**) torsion test.

The measured biomechanical test results of the *Camellia oleifera* flower bud are summarized in Table 2.

The biomechanical properties of *Camellia oleifera* flower bud show that the average values of the tensile force, shear force, and torsional moment of the collected *Camellia oleifera* flower bud were 8.968 N, 13.94 N, and 0.0178 N·m, respectively, and the maximum values of the tensile force, shear force, and torsional moment were 13.22 N, 16.32 N, and 0.0268 N·m, respectively.

Table 2. Summary of biomechanical properties of *Camellia oleifera* flower bud.

Group No.	Longitudinal Tensile Force/N			Shear Force/N	Internal Torque/N·m		
Flowers Period	**Bud Cracking**	**Initial Opening**	**Petal Standing**	**Any Flowers Period**	**Bud Cracking**	**Initial Opening**	**Petal Standing**
1	8.4 [1]	9.98	7.34	14.28	0.021	0.0114	0.0174
2	6.78	11.92	7.14	13.48	0.0252	0.0134	0.021
3	7.62	11.02	7.66	12.46	0.0254	0.0114	0.0164
4	8.22	11.08	7.96	13.5	0.0236	0.01	0.0174
5	7.4	13.22	9.06	14.68	0.0248	0.01	0.0214
6	8.44	10.56	8.4	16.32	0.0254	0.0104	0.0186
7	7.86	10.98	7.4	13.22	0.0268	0.0114	0.0188
8	6.94	11.24	7.84	12.36	0.019	0.0132	0.017
9	8.86	10.84	7.18	16.24	0.024	0.0104	0.0202
10	8.56	10.22	8.92	12.9	0.0256	0.011	0.0136
Average	7.908 [2]	11.106 [2] 8.968 [3]	7.89 [2]	13.94 [2]	0.0241 [2]	0.0113 [2] 0.0178 [3]	0.0182 [2]

[1] Each measurement in the table is the average of 10 *Camellia oleifera* flowers measurements from the same tree. [2] The average value is the average value of data from 1 to 10 in this column. [3] The average is the average of the three periods in the previous column.

2.2. *Camellia oleifera Flower Bud Collecting Actuator Design*

At present, there is no mechanical equipment to collect *Camellia oleifera* flower bud. Based on the results of the biomechanical measurements of *Camellia oleifera* flower bud in Section 2.1, three different types of *Camellia oleifera* flower bud collecting actuators were designed to collect *Camellia oleifera* flower bud by tensile force, shear force, and rotation torque, respectively. Through structural design and feasibility analysis, when all three collecting actuators can provide more than the removal force or torque measured in Section 2.1, they can be verified by processing test prototypes.

2.2.1. Triple-Finger Linkage Collecting Actuator

The triple-finger linkage collecting actuator utilizes longitudinal tensile force to remove the *Camellia oleifera* flower bud from the branch [7–9]. The structure is shown in Figure 4, with an electric push rod (9) hinged on a static platform (2), a hole in the middle of the static platform, and mounted with a conveying pipe (1). The electric actuator (9) pushes the synchronizing ring (8) upward, driving three C-links (6) along the frame (7) to move the three L-fingers (5) closer together, and the strut (3) and a locking ring (4) play an auxiliary role. The collection of the flower bud dislodged by tensile force is accomplished through the conveying pipe.

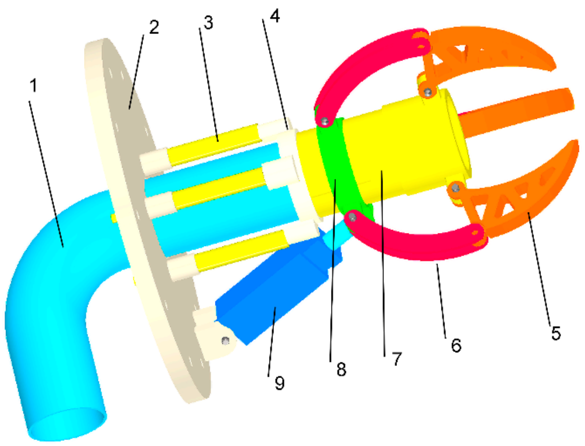

Figure 4. The design drawing of the triple-finger linkage collecting actuator. 1—Conveying pipeline, 2—static platform, 3—stub, 4—locking ring, 5—L-finger, 6—C-link, 7—rack, 8—synchronizing ring, 9—Electric push rod.

The mechanism is a symmetrical structure, and only one finger movement needs to be analyzed. The schematic diagram of the mechanism movement is shown in Figure 5.

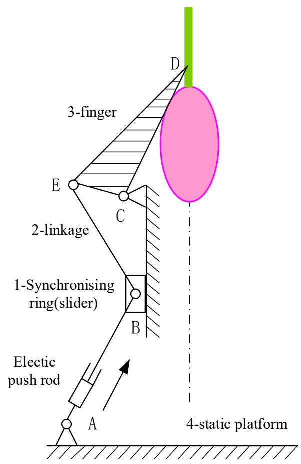

Figure 5. Mechanism motion schematic of the triple-finger linkage collecting actuator.

According to the analysis of the mechanism, the electric push rod only provides the drive, and the whole mechanism is a planar four-bar mechanism with the slider as the prime mover, which consists of the frame, connecting linkage, and finger. There are three movable members, one moving vice, and three rotating vices: B, C, and E. The degree-of-freedom equation of the mechanism is:

$$F = 3n - 2p_L - p_H = 3 \times 3 - 2 \times 4 - 0 = 1, \tag{1}$$

The number of primary moving parts of the mechanism is equal to the number of degrees of freedom, which satisfies the conditions of the mechanism to determine the motion. The force analysis of the slider, linkage, and finger are carried out, and all the components are 3D printed, ignoring their own gravity, as shown in Figure 6.

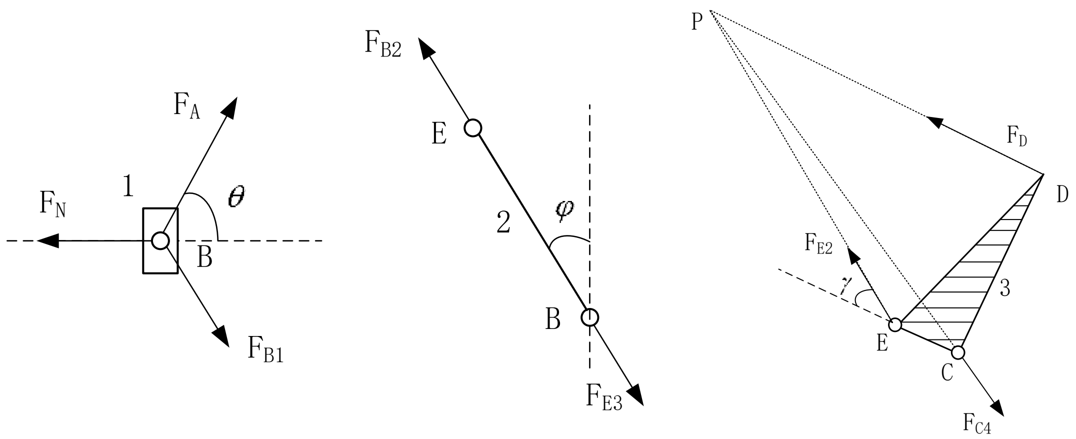

Figure 6. Component force diagram of the triple-finger linkage collecting actuator: (**a**) slide, (**b**) linkage, and (**c**) finger.

The force and torque balance equations for components 1, 2, and 3 are as follows:

$$\begin{cases} F_A \sin\theta - F_{B1} \cos\varphi = 0 \\ F_{B1} = F_{B2} = F_{E2} = F_{E3} \\ F_{E2} \sin\gamma \cdot l_{CE} = F_D \cdot l_{CD} \end{cases}, \tag{2}$$

F_A denotes the driving force of the electric actuator; F_B denotes the interaction force between slider 1 and the linkage, denoted as F_{B1} and F_{B2}, respectively; F_C denotes the force between finger 3 and frame 4; F_D denotes the reaction force exerted on finger 3 after the *Camellia oleifera* flower bud have been clamped; F_E denotes the interaction force between linkage 2 and finger 3, denoted as F_{E2} and F_{B3}, respectively; and l_{CE}, l_{CD} denote the length of the corresponding rod.

The point of application of the clamping force is point D at the end of the finger, and the feasibility of the model to collect the flower bud is judged based on the value of F_D. Under the driving force F_A, the force between the finger and the flower bud is F_D, and the force transfer ratio i is:

$$i = \frac{F_D}{F_A} = \frac{F_{E2}\sin\gamma \cdot l_{CE}\sin\theta}{l_{CD}F_{B1}\cos\varphi} = \frac{\sin\gamma \cdot l_{CE}\sin\theta}{l_{CD}\cos\varphi}, \tag{3}$$

Based on the geometric dimension derivation, several trigonometric functions in Equation (3) can be obtained as follows:

$$\begin{cases} \sin\theta = \frac{L_{AB}}{H_{AC}-l_{BC}} \\ \cos\varphi = \frac{{l_{BC}}^2+{l_{BE}}^2-{l_{CE}}^2}{2l_{BC}\cdot l_{BE}} \\ \sin\gamma = \sqrt{1-\left(\frac{{l_{CE}}^2+{l_{BE}}^2-{l_{BC}}^2}{2l_{BE}l_{CE}}\right)^2} \end{cases}, \tag{4}$$

l_{AB}, l_{AC}, l_{BC}, l_{BE} denote the length of the corresponding rod, L_{AB} denotes the distance between the lengths of the corresponding points A and B in the horizontal direction, and H_{AC} denotes the distance between the lengths of the corresponding points A and C in the vertical direction.

$$i = \frac{F_D}{F_A} = kl_{BC} + \text{constant term}, \tag{5}$$

Equation (5) shows that the force transmission ratio is proportional to the displacement of the slider, the slider moves to the farthest end of the displacement, and the finger clamping force is at its maximum. The designed rod length is $l_{BE} = 68$ mm, $l_{CE} = 28$ mm and the electric push rod drive force $F_A = 80$ N, yielding the maximum displacement of the slider when the force $F_D \approx 60$ N, which is far greater than the test measured tensile force of 8.968 N. This shows that the triple-finger linkage collecting actuator in the role of tensile force is able to separate *Camellia oleifera* flower bud from the branch.

2.2.2. Shear Type Collecting Actuator

The shear-type collecting actuator utilizes lateral shear force to remove the *Camellia oleifera* flower bud from the branch. As shown in Figure 7, when collecting flower bud, the three curved knife claws are merged to form a hemispherical space, and the spikes are machined to a thin edge, which can carry out the separation of flower bud and branches without harming the flower bud by relying on the shear force of the merging [10–13].

The mechanism is $F = 1$ and has deterministic motion. The movement sketch of the mechanism of the curved knife claw is shown in in Figure 8. B1 and B2 are the limit positions of the slider movement, the three curved knife claws are brought together at point D in the upper limit position, and a shear force of the same size is applied to cut the flower stem.

The mechanism is split into a basic mechanism with $F = 1$ and basic Assur group with $F = 0$. The force schematic is shown in Figure 9.

Taking the curved jaw 3 as the object of study, the closed force vector graph is drawn as shown in Figure 10.

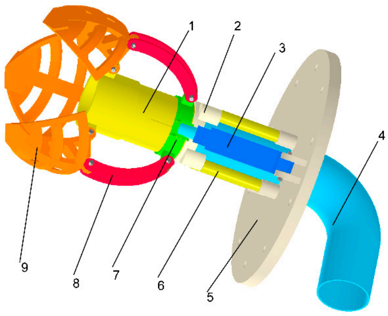

Figure 7. The design drawing of the shear-type collecting actuator. 1—Rack, 2—locking ring, 3—electric push rod, 4—conveying pipeline, 5—static platform, 6—stub, 7—synchronizing ring racks, 8—C-link, 9—three curved knife claws.

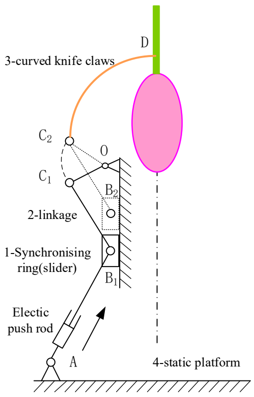

Figure 8. Mechanism motion schematic of the shear-type collecting actuator.

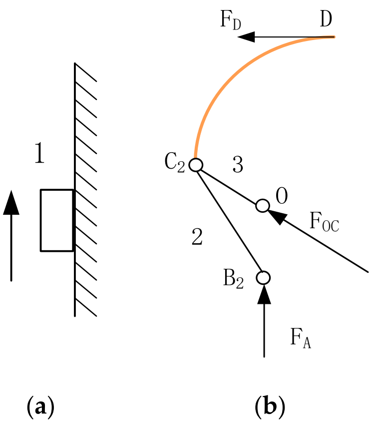

Figure 9. Force diagram of basic mechanism 1 and Assur groups 2–3 of the shear-type collecting actuator: (**a**), $F = 1$ basic mechanism, and (**b**) $F = 0$ II Assur groups.

The vector equation for the force of component 3 is as follows:

$$\vec{F_{OC}} = \vec{F_{BC}} + \vec{F_D}, \quad (6)$$

According to the triangle formula, the following numerical relationships between the three forces and three angles in the vector in Equation (6) are obtained:

$$\begin{cases} \frac{F_{OC}}{\sin\varphi} = \frac{F_{BC}}{\sin\gamma} = \frac{F_D}{\sin\theta} \\ \gamma = 180^\circ - \theta - \varphi \end{cases}, \quad (7)$$

$$F_D = \frac{F_{BC}\sin\theta}{\sin\gamma} = \frac{F_{BC}\sin\theta}{\sin(180^\circ - \theta - \varphi)} \quad (8)$$

where F_{BC} is the component force of F_A. The relation is $F_{BC} = \frac{F_A}{\cos \angle C_2B_2O}$, and $\angle\varphi = \angle C_2B_2O + 90°$.

The design rod length is $l_{BC} = 68$ mm, $l_{OC} = 28$ mm, $l_{CD} = 70$ mm, and the dimensions and angles of the limit positions are:

$$l_{B_1B_2} = 27.32\text{mm}, \angle C_2B_2O = 18.1°, \angle\theta = 30.7°, \angle\varphi = 108.1°.$$

The simplified shear force equation is obtained:

$$F_D = \frac{F_A \sin\theta}{\cos(\varphi - 90°)\sin(180° - \theta - \varphi)} = \frac{F_A \sin 30.7°}{\cos 18.1° \sin 41.2°}, \quad (9)$$

Therefore, under the force of electric push rod $F_A = 80$ N, the calculation of the shear force $F_D \approx 72$ N, which is much larger than the measured shear force of 13.94 N. This indicates that the shear-type collecting actuator is able to carry out shear separation of *Camellia oleifera* flower bud from the branch.

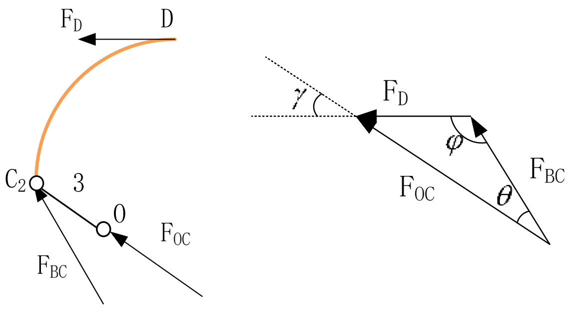

(**a**) (**b**)

Figure 10. Component 3 force diagram and force vector illustration of the shear-type collecting actuator: (**a**) Component 3 force analysis, and (**b**) Component 3 force vector.

2.2.3. Rotary Twist Collecting Actuator

A rotary-twist collecting actuator utilizes torsional torque to remove *Camellia oleifera* flower bud from the branch [2,9,14]. As shown in Figure 11, the rotary twist collecting actuator has a collection port set at the front and a delivery tube set at the back. A rotating conical friction roller is provided internally, leaving a channel in the center to connect with the collection port and the delivery tube.

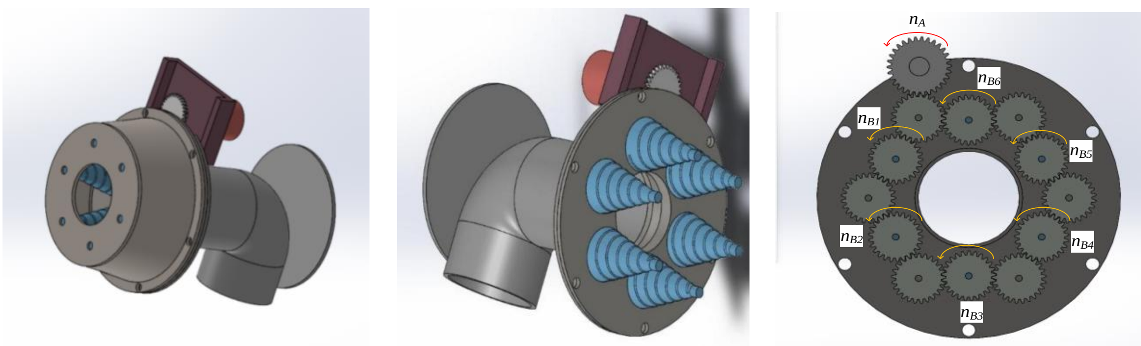

(**a**) (**b**) (**c**)

Figure 11. The design drawing of the rotary-twist collecting actuator: (**a**) Integral structure, and (**b**) Roller structure, and (**c**) Gear structure.

The collecting actuator adopts one $z = 68$ gear drive and twelve $m = 0.5, z = 36$ gear drive. Six gears with the same rotation direction as big gear A drive a friction roller to carry out the flower bud collection.

Taking two rollers on a straight line and the *Camellia oleifera* flower bud as the research object, the center of the flower bud is the center of the circle, the direction of the connecting line with the first and fourth rollers is the X-axis, the diameter direction is the contact of the three circles, and the axial direction is the contact of one circle with two isosceles trapeziums, as shown in Figure 12.

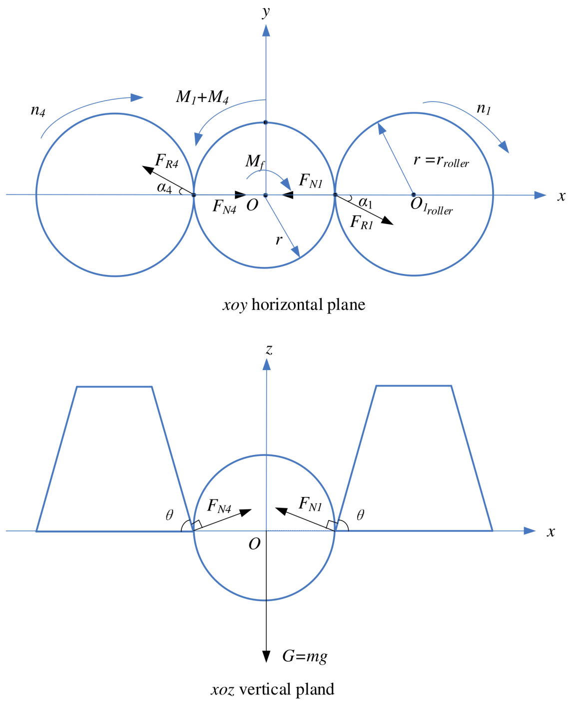

Figure 12. Schematic diagram of the stress model of *Camellia oleifera* flower bud of the rotary-twist collecting actuator.

Considering the force equilibrium of the *Camellia oleifera* flower bud, the force equation is:

$$\begin{cases} F_{Nx} = F_{N1}\sin\theta + F_{N4}\sin\theta = F_{R1}\cos\alpha_1 + F_{R4}\cos\alpha_4 \\ F_{Nz} = 6F_{N1}\cos\theta = G \end{cases} \quad (10)$$

where F_{N1}, F_{N4} denote the normal force exerted on the flower bud by the first and fourth rollers, respectively; F_{R1}, F_{R4} denote the total reaction force of the bud acted by the first and fourth rollers, respectively; α_1, α_4 denote the angle between the total force of the flower bud and the X-axis, respectively, as 30°; G denotes the gravity of the flower bud,$G = mg \approx 20$ N; and θ denotes the trapezoidal angle of the rollers, and all rollers are 60°.

Collating Equation (10), the formula for the horizontal component of the normal force exerted by the roller on the *Camellia oleifera* flower bud is obtained as:

$$F_{Nx} = \frac{1}{3}G\tan\theta \quad (11)$$

The *Camellia oleifera* flower bud fall under the twisting of the roller, and the torque is equal to the resistance torque between the flower bud and the branch M_f. The roller is uniformly distributed along the circumference of the circle, and the normal force and the rotating torque of the six rollers are equal to obtain the equilibrium equations of the torque of the *Camellia oleifera* flower bud:

$$\begin{cases} M_f = 6(M_1 + rF_{R1}\sin\alpha_1) \\ F_{R1}\cos\alpha_1 = F_{R4}\cos\alpha_4 = F_{N1}\sin\theta = F_{N4}\sin\theta \end{cases} \quad (12)$$

M_f denotes the resistance torque generated by the contact of the *Camellia oleifera* flower bud with the branches, and M_1 denotes the rotational torque exerted by the first roller, $M_1 = M_4 = J\beta$.

$$M_f = 6M_1 + \frac{r}{6}G\tan\theta\tan\alpha_1, \tag{13}$$

The roller is a hollow conical table with uniformly distributed mass $m = 2g$, a bottom radius r_{roller}= 20 mm, a rotary inertia $J_z = \frac{1}{2}m{r_{\text{roller}}}^2$, and an angular acceleration $\beta = \frac{d\omega}{dt}$. Then, the resisting torque of the *Camellia oleifera* flower bud collection is derived as:

$$M_f = 3m{r_{\text{roller}}}^2\frac{d\omega}{dt} + \frac{r}{6}G\tan\theta\tan\alpha_1 \tag{14}$$

The rotary-twisting collecting actuator has three pairs of rollers, and flower bud collection can be achieved when the rotational torque M_{roller} during operation is greater than or equal to $\frac{1}{3}$ of the resistance torque M_f:

$$M_{\text{roller}} = \frac{1}{3}M_f = m{r_{\text{roller}}}^2\frac{d\omega}{dt} + \frac{r}{6}G\tan\theta\tan\alpha_1 \tag{15}$$

2.3. *Camellia oleifera Flower Bud Collecting Actuator Design Summary*

The three types of collecting actuators adopt different structures to provide corresponding types of forces. The triple-finger linage collecting actuator and the shear-type collecting actuator provide pulling force and shearing force, respectively, to remove the flower bud from the branches of *Camellia oleifera*. The proposed rotary-twist collecting actuator relies on the torsional moment to separate the flower bud from the branch, which is an innovative principle.

3. Simulation Results

The value of the rotational torque when the rotary-twist collecting actuator is working can be obtained by dynamics simulation. The rotary-twist collecting actuator model was imported into ADAMS2021 (Automatic Dynamic Analysis of Mechanical Systems, Pittsburgh, PA, USA) software and constraints were added [15,16], as shown in Figure 13.

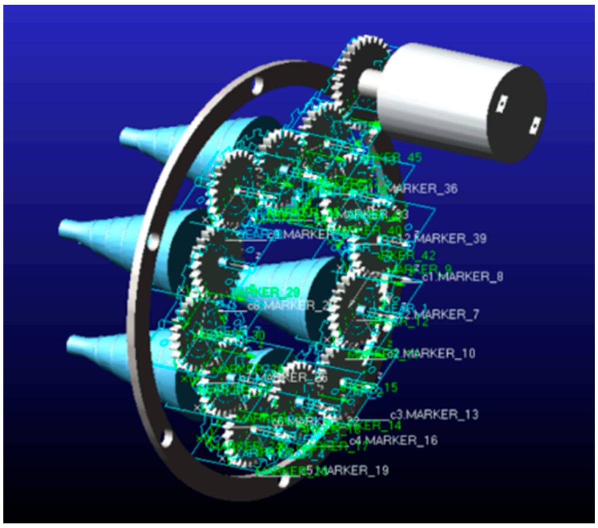

Figure 13. Dynamic model of the rotary-twisting collecting actuator.

In the mode, the roller and the gear are rigidly connected, the gear is 45 steel, the Poisson's ratio is 0.27, the Young's modulus is 2.07×10^{11} PA, the load is 0.01 N·m, the motor speed is 400 r/min, the simulation time is 1 s, and the time step is 0.001 s, and the simulation obtained the torque curve of the roller, as shown in Figure 14.

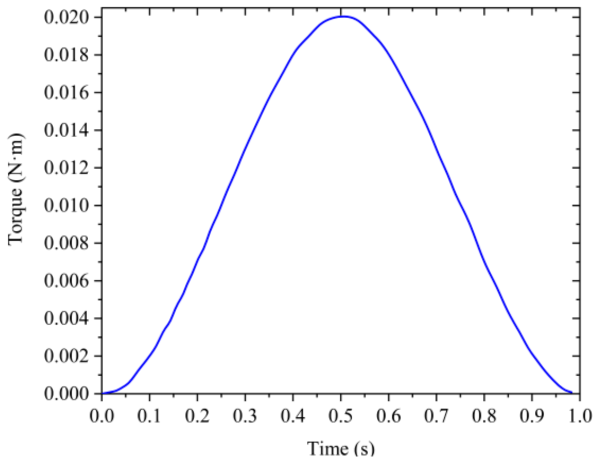

Figure 14. Roller torque curve of the rotary-twisting collecting actuator.

The roller torque could be quickly and smoothly increased to M_{roller}= 0.02 N·m. This value was greater than the test determination of the *Camellia oleifera* flower bud collection, which required a torsional torque of 0.0178 N·m, so when setting the rotary-twist type collecting actuator of the motor speed for the 400 r/min, the collecting actuator could achieve the collection of the required torque.

4. Test Results

4.1. Materials and Methods

Three types of collecting actuators were processed in prototype machines and the *Camellia oleifera* flower bud collection test was carried out. Both the triple-finger linkage type and the shear-type were driven by electric push rods with a thrust of $F_A = 80$ N. The maximum speed of the rotary motor was 400 r/min, and the collecting process is shown in Figure 15. Ten *Camellia oleifera* trees were randomly selected and 10 flower bud were labeled for collection. Three sets of 10 × 10 collection results were recorded [17–20].

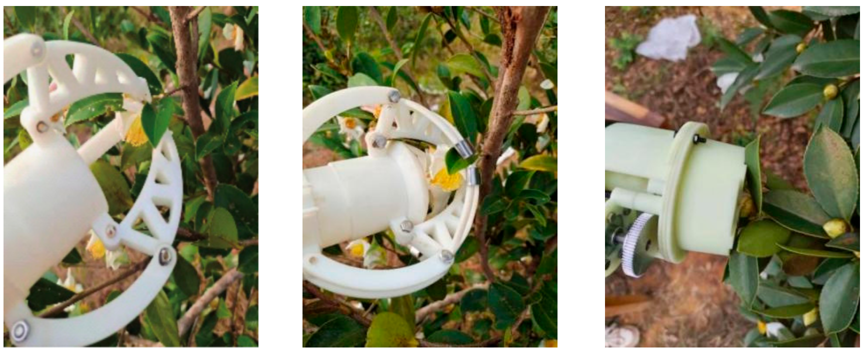

(**a**) (**b**) (**c**)

Figure 15. Collecting test of three types of collecting actuators: (**a**) Triple-finger linkage collecting actuator, (**b**) Shear-type collecting actuator and (**c**) Rotary twist collecting actuator.

Using the high-speed microscope camera of the Canadian Norpix brand FR Stream 3F model, videos of *Camellia oleifera* flower bud in pipelines were captured and transported using the complete pipeline as the basis for successful collection. A photo was taken to obtain the number of successfully collected flower bud and the collection time, as shown in Figure 16. The number of *Camellia oleifera* flower bud in the collection box was counted after collection, and the number of flower bud with damaged appearance or damaged stamens was recorded. The photos of the *Camellia oleifera* flower bud after collection are shown in Figure 17.

(a) (b) (c)

Figure 16. *Camellia oleifera* flower bud collection and transportation photos:(**a**) Starting position, (**b**) Middle position, and (**c**) End position.

Figure 17. The collected *Camellia oleifera* flower bud in the collection box.

4.2. Results and Discussion

The collection success rate and bud breakage rate were selected as test indexes in this collection test, which are defined as follows:

Collection success rate: If the number of flower bud collected by the collecting actuator in a single test is n_1, and the number of flower bud not collected in a single collection is n_2, then the collection success rate is:

$$y_1 = \frac{n_1}{n_1 + n_2}, \tag{16}$$

Bud breakage rate: If the number of broken flower bud collected in a single test is n_3, and the number of intact flower bud is n_4, then the bud breakage rate is:

$$y_2 = \frac{n_3}{n_3 + n_4} \tag{17}$$

The collection test results are summarized in Table 3.

The triple-finger linkage collecting actuator, shear-type collecting actuator, and rotary-twist collecting actuator collected single *Camellia oleifera* flower bud with an average time of 4.58 s/bud, 5.15 s/bud, and 1.57 s/bud, respectively. The collection success rate for one operation was 59%, 49%, and 91%, respectively. The bud breakage rate was 7.6%, 5.4%, and 4.9%, respectively. As shown in Figure 18, the rotary twist collecting actuator had the shortest collection time, the highest collection success rate, and the lowest bud breakage rate, which has obvious advantages.

Table 3. Test results of the different kinds of collecting actuators.

Collecting Actuator Type	Triple-Finger Linkage			Shear Type			Rotary Twist		
	Collection Time (s/Bud)	Collection Success Rate	Bud Breakage Rate	Collection Time (s/Bud)	Collection Success Rate	Bud Breakage Rate	Collection Time (s/Bud)	Collection Success Rate	Bud Breakage Rate
1	4.87 [1]	60%	8%	5.50	50%	5%	1.62	90%	5%
2	4.62	70%	9%	5.22	60%	5%	1.48	100%	5%
3	4.34	70%	7%	5.08	50%	6%	1.56	90%	5%
4	4.55	60%	6%	4.95	60%	6%	1.72	90%	4%
5	4.21	50%	6%	5.32	50%	4%	1.84	90%	5%
6	4.20	50%	8%	5.05	40%	5%	1.45	90%	5%
7	4.82	60%	8%	5.12	50%	6%	1.53	100%	5%
8	4.66	60%	7%	5.33	40%	6%	1.49	90%	5%
9	4.86	50%	9%	4.88	40%	6%	1.52	90%	5%
10	4.67	60%	8%	5.05	50%	5%	1.49	80%	5%
Average value	4.58 [2]	59%	7.6%	5.15	49%	5.4%	1.57	91%	4.9%

[1] Each measurement in the table is the average of 10 *Camellia oleifera* flower measurements from the same tree.
[2] The average value is the average value of data from 1 to 10 in this column.

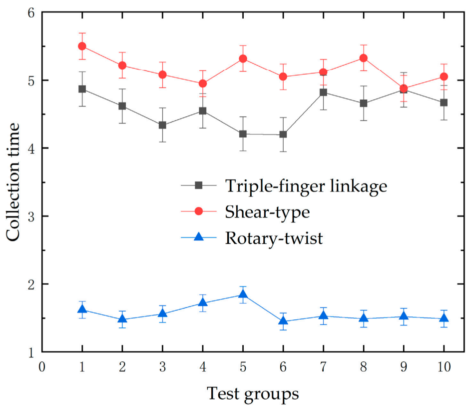

(**a**)

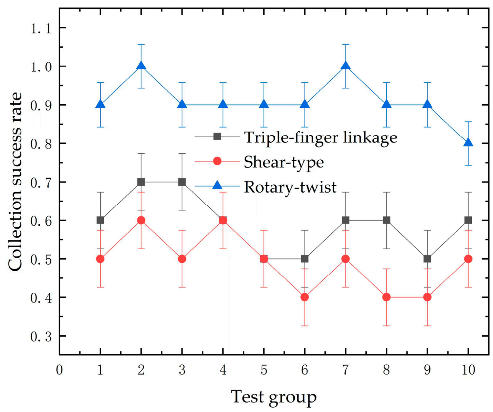

(**b**)

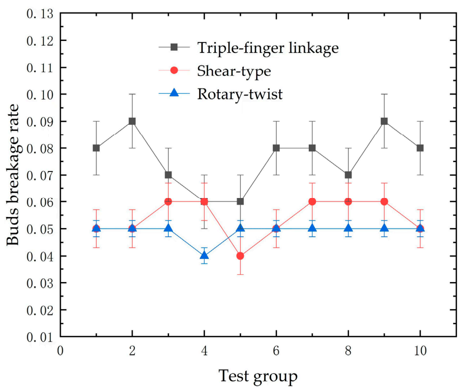

(**c**)

Figure 18. The results of the three types of collecting actuators: (**a**) collection time, (**b**) collection success rate, and (**c**) bud breakage rate.

The statistical results of the collecting test were compared with the biomechanical data of the *Camellia oleifera* flower bud. The longitudinal tensile force of *Camellia oleifera* flower bud was 8.968 N, the transverse shear force was 5.73 N, and the transverse torsional torque was 0.0178 N·m. It was found that the greater the removal force or moment, the longer the collection time. The values of longitudinal tensile force and transverse shear force were high, so it took a long time to collect *Camellia oleifera* flower bud, and the collection success rate was not high. The triple-finger linkage collecting actuator had the highest breakage rate, because it was easy to cause the flower bud to break when pulling the flower bud. The shear-type collecting actuator had the middle breakage rate, which indicates that the shear force was more suitable than the tensile force during flower bud collection.

The torsional moment of *Camellia oleifera* flower bud removed from the branch measured by the previous biomechanical test was the smallest, the time spent collecting *Camellia oleifera* flower bud with the rotary-twisting collecting actuator was the shortest, the collection success rate was higher than 90%, and the breakage rate was lower than 5%. Therefore, the rotary-twisting collecting actuator is the best choice for collecting *Camellia oleifera* flower bud with high efficiency and low loss.

5. Conclusions

In view of the current situation that there is no mechanical equipment for *Camellia oleifera* flower bud collection, the research goal is to develop a collecting actuator. In this paper, three types of collection actuators based on the biomechanical characteristics were designed. Through mechanical analysis and dynamic simulation, the power parameters of three types of collecting actuators were obtained. Through the test of collecting *Camellia oleifera* flower bud, it was verified that the collection time of the rotary-twist collecting actuator was 1.57 s, the collection success rate was 91%, and the bud breakage rate was 4.9%. The rotary-twist collecting actuator can achieve efficient and low-loss collection of *Camellia oleifera* flower bud. In the next step, the rotary-twist collecting actuator can be combined with a forestry robot to continue the research on *Camellia oleifera* flower bud collecting robots.

6. Patents

In this paper, the research results for the rotary-twist collecting actuator have been granted a Chinese invention patent (ZL202111520489.1).

Author Contributions: Writing—review and editing, Q.Z.; writing—original draft preparation, Q.Z.; conceptualization, Q.Z. and L.L.; methodology, L.L.; software, L.L.; validation, Q.Z., L.L. and Z.Y.; formal analysis, Z.Y.; investigation, Z.Y.; resources, Z.Y.; data curation, Q.Z.; project administration, L.L.; funding acquisition, L.L. All authors have read and agreed to the published version of the manuscript.

Funding: In this paper: The research was supported by the National Key R&D Program of China (No. 2022YFD2202103), the State Forestry and Grassland Equipment Science and Technology Innovation Park Research Program of China (No. 2023YG053), and the College Students' Innovation and Entrepreneurship Training Program of Central South University of Forestry and Technology (No. S202310538082).

Data Availability Statement: The original contributions presented in the study are included in the article, further inquiries can be directed to the corresponding author.

Acknowledgments: The authors would like to thank the research team members for their contributions to this work.

Conflicts of Interest: The authors declare no conflicts of interest.

References

1. Hu, J.; Liu, F.; Qin, J. The Recent Advances in Research on Effective Pollinators of Camellia Oleifera. *J. Bee* **2019**, *39*, 27–30.
2. Wen, Y.; Zhang, Y.; Su, S.; Yang, S.; Ma, L.; Zhang, L.; Wang, X. Effects of Tree Shape on the Microclimate and Fruit Quality Parameters of *Camellia oleifera* Abel. *Forests* **2019**, *10*, 563. [CrossRef]
3. Wang, X.N.; Chen, Y.Z.; Wang, R.; Peng, S.F.; Chen, L.S.; Ma, L.; Tang, W.; Luo, J. Flowering and pollinating specifications of *Camellia oleifera* cultivars. *J. Cent. South Univ. For. Technol.* **2013**, *33*, 1–6+181.
4. Chen, Y.; Yuan, D.Y.; Li, K.; Yang, Y.H.; Jin, Y.J.; Lin, M.H.; Zhou, F. Viability Determination and Preservation of Pollen of *Camellia oleifera* 'Huashuo', 'Huaxin' and 'Huajin'. *Acta Agric. Univ. Jiangxinensis* **2020**, *42*, 118–126.
5. Willoughby, R.A.; Solie, J.B.; Whitney, R.W.; Maness, N.O. A mechanized harvester for marigold flowers. In Proceedings of the ASAE International Meeting, Milwaulkee, WI, USA, 9–12 July 2000; pp. 1–14.
6. Wang, J.Z.; Guan, W.; Yang, L.P.; Zhang, J.T.; Liu, S.H. Design and Analysis of Rose Harvesting Robot End-effector. *Ind. Control Comput.* **2021**, *34*, 68–69+71.

7. Wu, Z.C.; Zhao, Q.; Li, L.J.; Guo, X.; Li, J. Study on the design of three-claw linkage type camellia flower picking execution terminal. *Chin. J. Constr. Mach.* **2022**, *20*, 69–74+80.
8. Wang, Y.; Zhang, M.; Liu, B.; Liu, S.; He, Y.; Xu, H.B. Desigh and Experiment of Clamping Mechaism about End-effector for Citrus Harvesting Robot. *J. Agric. Sci. Technol.* **2019**, *21*, 61–69.
9. Wang, Y.; Fu, S.; Zhang, Z.; Ma, J.T.; Xu, H.B. Design and Experimentation on End-effector of Citrus Picking Robot. *J. Agric. Sci. Technol.* **2018**, *20*, 69–77.
10. Lv, H.; Li, L.J.; Zhao, Q.; Wu, Z.C.; Guo, X. Design and Experiment of Cutting End Effector for Camellia Picking. *J. Agric. Mech. Res.* **2024**, *4*, 134–139+144.
11. Liu, P.L. Research and Design of An Apple-Picking Robot. Master's Thesis, Xi'an University of Technology, Xi'an, China, 2018.
12. Zhou, S.L. A Study of Cucumber Picking Manipulator on Structural Optimization and Machine Vision. Master's Thesis, Jilin University, Jilin, China, 2019.
13. Wang, L.L. Research on Key Technology of Tomato Havesting Robot. Ph.D. Thesis, Beijing University of Technology, Beijing, China, 2018.
14. Gaoy, H. Research on Key Techniques of Strawberry Picking and Optimal Design of Manipulator. Master's Thesis, Shandong Agricultural University, Taian, China, 2021.
15. Chen, G.; Zhou, Q.; Wu, J.; Yan, N. Research for Co-simulation of 7 DOF Manipulator Based on Adams and MATLAB. *J. Syst. Simul.* **2020**, *29*, 99–106.
16. Kumar, V. Kinematics/Dynamics Analysis with ADAMS/MATLAB Co-Simulation of a SolidWorks Designed Spatial Robot Arm with Control and Validation of Results. In *Machines, Mechanism and Robotics: Proceedings of iNaCoMM 2019*; Springer: Singapore, 2022; pp. 1197–1209.
17. Wu, Z.; Li, L.; Zhao, Q.; Guo, X.; Li, J. Design and Research of a Harvesting Actuator for *Camellia oleifera* Flowers during the Budding Period. *Agriculture* **2022**, *12*, 1698. [CrossRef]
18. Wang, R.; Zheng, Z.; Zhu, G.; Gao, L.; Cui, B. Research status of harvesting machines for medicinal flowers. In Proceedings of the ASABE Annual International Meeting, Boston, MA, USA, 7–10 July 2019.
19. Qin, J.; Yin, Y.; Liu, Z.; Du, Y.; Wang, G.; Zhu, Z.; Li, Z. Optimization of maize picking mechanism by simulation analysis and high-speed video experiments. *Biosyst. Eng.* **2020**, *189*, 84–189. [CrossRef]
20. Li, J.; Zhao, Q.; Li, L.J.; Wu, Z.C.; Guo, X. Trajectory Planning of Camellia oleifera pollen picking manipulator based on Improved Particle Swarm Optimization Algorithm. *J. Mech. Transm.* **2023**, *47*, 86–92.